This article has been accepted for publication in a future issue of this journal, but has not been fully edited. Content may change prior to final publication. Citation information: DOI 10.1109/TMM.2018.2820327, IEEE Transactions on Multimedia

Super-pixel Based Single Nighttime Image Haze Removal

Minmin Yang, Jianchang Liu, and Zhengguo Li, *Senior Member, IEEE*

***Abstract*—Haze removal is important to improve performance of out-door vision systems. However, it is challenging to remove haze from a single nighttime haze image. In this paper, a novel super-pixel based single image haze removal algorithm is proposed for nighttime haze images. The input nighttime image is first decomposed into a glow image and a glow-free nighttime haze image using their relative smoothness. A super-pixel based method is then introduced to compute the value of atmospheric light and dark channel for each pixel in the glow-free haze image. The transmission map is decomposed from the dark channel of the glow-free haze image by the weighted guided image filter. Since super-pixels usually adhere to the boundaries of objects well, a smaller local window size can be selected. As such, details in areas of fine structures are preserved better. In addition, to avoid noticeable noise in the sky area, an adaptive threshold is added to the transmission map when the nighttime haze image is restored. Experiments show that our method produces better results than existing haze removal algorithms for nighttime haze images.**

***Index Terms*—Nighttime image haze removal, Glow decomposition, Morphologic artifacts, Super-pixel segmentation, Weighted guided image filtering.**

I. Introduction

IN real life, natural phenomena (such as rain, haze, snow etc.) can easily lead to degradation of outdoor images. Because in these environments, large amounts of particles floating in the atmosphere, light propagation in the atmosphere will be affected by these floating particles. In the field of computer vision, image dehazing has a wider demand. From the perspective of image processing, it can provide a pretreatment for some visual algorithms. Besides, from the practical point of view, it plays an important role in military system and civil system [1]. Haze-free images make the scene look more realistic and provide more useful information. Therefore, the research of image dehazing has important practical significance and development prospect.

There have been many haze removal methods which are based on the optical model developed for daytime haze images. At present, the most widely physical model is a linear equation consisting of transmission and atmospheric light. According to the model, daytime dehazing methods need to estimate the atmospheric light and transmission map. Many classic methods use additional information or multiple pictures to remove haze from the haze images. For example, Schechner et al. [2] proposed a novel method of using images with different polarizer orientations to dehazing. Lai et al. [3] proposed an interesting method to derive the optimal transmission map directly from the daytime haze image model. It was shown in [3] that finding the optimal transmission is equivalent to solve a constrained minimization problem by quadratic programming. It should be pointed out that the goal of [3] is to recover the underlying scene radiance rather than to maximize the visibility.

In [4], a fast algorithm for single image dehazing is proposed based on linear transformation by assuming that a linear relationship exists in the minimum channel between the hazy image and the haze-free image. On top of dark channel prior, He et al. introduced a simple method to study single image haze removal in [5]. The dark channel prior is based on an observation that most local patches in haze-free scene images contain some pixels which have very low intensities in at least one color channel. Many dark channel prior based haze removal algorithms were introduced since then [7] [8]. The dark channel prior based methods usually work well, but the dark channel prior has limitations. For example, morphological artifacts are an issue for the dark channel prior when the initial transmission map is computed using the dark channel prior [5]. Moreover, as pointed out in [5], the dark channel prior is not always true. A simple edge preserving decomposition based framework was proposed for single image haze removal in [9]. The simplified dark channel of the haze image is decomposed into a base layer and a detail layer via the weighted guided image filter (WGIF) in [11], and the transmission map is estimated from the base layer. Image enhancement-based methods are also applied to the image dehazing, for example [12] [13] [14].

Even though these methods generally perform well for daytime haze images, they are not well equipped to correct nighttime scenes due to varying imaging conditions such as active light sources or glow effects. Due to existences of active light sources, for example, street lights et al, and their associated glow, the model of daytime haze images are not applicable to the nighttime haze images.

Recently, several interesting methods were emerged to enhance nighttime haze images [15] [16] [17] [20]. Pei and Lee [15] introduced a method based the color transfer processing. The colors of a nighttime haze image were mapped to those of a daytime haze image. Then, a dark channel prior based algorithm was provided to estimate the transmission map. A post-processing step was also provided to improve the insufficient brightness and low overall contrast of haze-free

M. Yang and J. Liu are with the College of Information Science and Engineering, Northeastern University, and the State Key Laboratory of Synthetical Automation for Process Industries, Northeastern University, Shenyang, Liaoning Province, 110819, P. R. China; e-mail: ymm_2011@163.com; liujianchang@ise.neu.edu.cn.

Z. Li is with the Signal Processing Department, Institute for Infocomm Research, Singapore 138632; e-mail: ezgli@i2r.a-star.edu.sg.

1520-9210 (c) 2018 IEEE. Personal use is permitted, but republication/redistribution requires IEEE permission. See http://www.ieee.org/publications_standards/publications/rights/index.html for more information.

This article has been accepted for publication in a future issue of this journal, but has not been fully edited. Content may change prior to final publication. Citation information: DOI 10.1109/TMM.2018.2820327, IEEE Transactions on Multimedia

image. Due to the color transfer, although their method has the reliable dehazing quality, the color of the whole haze-free image looks unnatural. Zhang et al [16] proposed a new image model which accounted for varying illumination. First, the light intensity was estimated and enhanced to obtain an illumination balanced result, then, they estimated the color characteristics of the incident light, finally, they used the dark channel prior to remove the haze. Li et al [17] introduced a new nighttime haze model that accounts for the varying light sources and their glow. The model is a linear equation consisting of transmission map, atmospheric light and glow. The glow is first removed from the input image by using the layer separation technique in [23] and a glow-free nighttime haze image is obtained. The haze removal algorithm in [5] was then extended to remove haze from the nighttime haze image. The nighttime haze image is decomposed into a grid of small areas (15×15) and the brightest intensity in each local area is selected as the atmospheric light of the area. The dark channel prior is employed to estimate the transmission map. To reduce morphological artifacts that is caused by the grid and the local maximum or minimum operation, size of local windows in the guided image filter (GIF) has to be selected a large value like a circle with the radius as 60. It was pointed out in [18] that details in areas of fine structures are not preserved well by such a large local window. The algorithm can usually produce good results except for halo artifacts and amplified noise in some final images. Ancuti et al [20] proposed an effective technique builds on multi-scale fusion approach. The value of atmospheric light is estimated on image patch and not on the entire image. Although the haze can be removed from the nighttime image, the dehazed image still exists color distortion. Overall, it is desired to design a new haze removal algorithm based on the super-pixels of the haze image for night-time haze images.

In this paper, a novel super-pixel based algorithm is introduced to remove haze from a haze image captured at nighttime. The proposed method is based on the nighttime haze image model in [17]. The input image is first decomposed into a glow image and a glow-free nighttime haze image via solving a quadratic optimization problem. The proposed super-pixel based haze removal algorithm is then adopted to remove haze from the glow-free nighttime haze image.

There are two key components in the proposed algorithm. One is on the estimation of the atmospheric light and the other is on the computation of the transmission map. Instead of decomposing the glow removal image into a grid of small areas (15×15) and selecting the brightest pixel in each area as the local atmospheric light in [17], the nighttime haze image is divided into super-pixels and the super-pixels are chosen as the unit for the estimation of the local atmospheric right. The SLIC in [21] is adopted to segment a nighttime haze image into super-pixels. The brightest pixel color in each super-pixel is regard as this super-pixel's atmospheric light, and the atmospheric light is further refined by the WGIF. The transmission map is also estimated via a super-pixel based method. It was shown in [27] that all pixels in a super-pixel usually share the same depth. Thus, it is reasonable to assume that all pixels in a super-pixel usually share the same transmission map [10]. It should be pointed out that the dark channel is adopted in the proposed algorithm to reduce the variation range of the direct attenuation such that it becomes detail layer for the dark channel of the haze image. This is different from the existing dark channel prior which requires to cancel the direct attenuation from the dark channel of the haze image. The dark channel of the haze image is decomposed into two layers using the WGIF. The transmission map is computed from the base layer. Experimental results show that the proposed algorithm can be applied to achieve images with better visual quality than the existing nighttime haze removal algorithms in [16] [17]. On the other hand, due to using the SLIC to segment the image, the running time of the algorithm is relatively slower.

Overall, the main contribution of this paper is a new type of haze removal algorithm using the concept of super-pixel. Compared with the patch based methods, the super-pixel can be used to reduce morphologic artifacts caused by the patch. This is because that the super-pixels can adhere to boundaries of objects in the haze image well. As such, the radius of the WGIF can be reduced. Subsequently, more fine details can be preserved. In addition, the proposed super-pixel based method has more chance to accurately estimate the transmission maps for all pixels in white objects nearby a camera than the algorithms in [9], [17] and [25]. In other words, the proposed method provides a solution to a challenging problem on the estimation of transmission maps for pixels in white objects nearby the camera.

The rest of this paper is organized as follows: In section II, we briefly review the preliminary knowledge. In section III, we present the process of nighttime single image haze removal. In section IV and section V clarify results analysis and conclusion briefly.

II. Preliminary Knowledge

Since the WGIF and the SLIC will be applied in the proposed method, the relevant knowledge on them are summerized in this section.

A. Weighted Guided Image Filter

Denote the guidance image as I, the filtering output as Z, and the input image as X in [5] [6]. The images I and X could be identical. Z is assumed to be a linear transform of I in a window Ω_k centered at the pixel p, and the radius of the window Ω_k is r:

$$Z(p) = a_k I(p) + b_k, \forall p \in \Omega_k, \tag{1}$$

where the value of (a_k, b_k) can be computed by minimizing the following cost function in the window Ω_k [5]:

$$E(a_k, b_k) = \sum_{p \in \Omega_k} ((a_k I(p) + b_k - X_p)^2 + \lambda a_k^2), \tag{2}$$

and λ is a regularization parameter penalizing large a_k. Since, halo artifacts may appear on some edges, an edge-aware

1520-9210 (c) 2018 IEEE. Personal use is permitted, but republication/redistribution requires IEEE permission. See http://www.ieee.org/publications_standards/publications/rights/index.html for more information.

This article has been accepted for publication in a future issue of this journal, but has not been fully edited. Content may change prior to final publication. Citation information: DOI 10.1109/TMM.2018.2820327, IEEE Transactions on Multimedia

weighting is introduced and incorporated into the GIF to form the WGIF in [11]. The edge-aware weighting $\Gamma_I(k)$ is :

$$\Gamma_I(k) = \frac{1}{N}\sum_{p=1}^{N}\frac{\sigma_{I,r}^2(k)+\varepsilon}{\sigma_{I,r}^2(p)+\varepsilon}, \tag{3}$$

where N represents the number of pixels. The $\sigma_{I,r}(k)$ is the variance of I in the window Ω_k. The value of ε is assigned $(0.001L)^2$, and, L is the dynamic range of I. The cost function $E(a_k, b_k)$ is changed to:

$$E(a_k,b_k) = \sum_{p\in\Omega_k}((a_kI(p)+b_k-X(p))^2 + \frac{\lambda}{\Gamma_I(k)}a_k^2), \tag{4}$$

The solutions of a_k and b_k are given as:

$$a_k = \frac{\mu_{I\odot X,r}(k)-\mu_{I,r}(k)\mu_{X,r}(k)}{\sigma_{I,r}^2(k)+\frac{\lambda}{\Gamma_I(k)}}, \tag{5}$$

$$b_k = \mu_{X,r}(k) - a_k\mu_{I,r}(k) \tag{6}$$

where $\odot$ is the element-by-element product of two matrices. $\mu_{I\odot X,r}(k)$, $\mu_{I,r}(k)$ and $\mu_{X,r}(k)$ are the mean values of $I\odot X$, I and X, respectively. In this paper, we use the WGIF to refine the atmospheric light and the transmission map. It is well known that local filters such as the GIF and the WGIF have a fundamental limitation to preserve details in areas of fine structures. Recently, it was pointed out in [18] that one major reason is due to the large value of r.

The no-reference perceptual haze density assessment metric D in [19] is adopted to compare different selection of r in the WGIF by using it to study single image haze removal for a day-time haze image. The metric in [19] does not require the original haze image. When the values of D are small, the effect of dehazing will be better. The D values for the haze image, the dehazed image with r as 60, and the dehazed image with r as 20 are 1.6517, 0.8084 and 0.7723, respectively. In addition, it is shown in Fig. 1 that the structure of hair in the dehazed image with r as 20 is indeed preserved better.

(a) (b) (c)

Fig. 1: (a) haze image; (b) dehazed image with $r = 20$; (c) dehazed image with $r = 60$. More fine details are preserved by a smaller radius.

B. Super-pixel Segmentation Via The SLIC

A super-pixel is a small area composed by a series of pixels with adjacent positions, similar color, similar brightness, similar texture and other characteristics. Achanta et al. [21] proposed the concept of simple linear iterative clustering (SLIC), it is a common method of the super-pixel segmentation. This method can segment pixels quickly and simply, besides, it can identify boundaries better. The color images are transformed into a five-dimensional feature vectors $V = [l, a, b, x, y]$ in CIELAB color space and XY coordinate. Where, $[l, a, b]$ indicates the color of pixel, $[x, y]$ indicates the position of pixel. It is a distance measurement standard for five-dimensional feature vectors, and a local clustering process for image pixels. SLIC algorithm can generate compact and approximately uniform super-pixels. Besides, it has a high overall evaluation in terms of speed, contour preserving and hyper pixel shape, and the segmentation effect is in line with people's expectation.

The metric of SLIC is given as:

$$d_{lab} = \sqrt{(l(p)-l(p'))^2+(a(p)-a(p'))^2+(b(p)-b(p'))^2} \tag{7}$$

$$d_{xy} = \sqrt{(x(p)-x(p'))^2+(y(p)-y(p'))^2} \tag{8}$$

$$D_s = \sqrt{(\frac{d_{lab}}{N_{lab}})^2+(\frac{d_{xy}}{N_{xy}})^2} \tag{9}$$

where, d_{lab} indicates color distance; d_{xy} indicates spatial distance; p and p' are two pixels; $N_{xy} = \sqrt{\frac{K}{N}}$, where K is called the total number of pixels, N is the number of the super-pixels; N_{lab} varies with different images, but it is generally a fixed value. The super-pixels usually can identify boundaries better. So, it can be expected that the concept of super-pixel can be used to reduce the morphological artifacts in the single image haze removal. As such, size of local windows in the WGIF can be reduced. Subsequently, details in areas of fine structures can be preserved better.

III. Nighttime Single Image Haze Removal

In this section, we first provide details on the model of nighttime haze images. Based on this model, the glow is removed from the input image thereby the glow-free haze image is obtained. The model of the glow-free haze image is similar with the model of daytime haze image except that the atmospheric light is spatially varying in the nighttime haze image. It is thus expected that existing dark channel based algorithm for daytime haze removal can be extended to deal with nighttime haze image. Based on this observation, a super-pixel based haze removal algorithm is presented for the glow-free nighttime haze images. Two key components of the proposed algorithm are a super-pixel based method for the estimation of the atmospheric light and a super-pixel based approach for the estimation of the transmission map.

A. Modelling Of A Nighttime Haze Image

Since the light source only from the sun, the daytime images are not affected by other light sources. In the daytime haze image dehazing algorithm, the model is commonly used as:

$$X_c(p) = Z_c(p)t(p) + A_c(1-t(p)) \tag{10}$$

When a picture is captured at night, light sources mainly come from street lights and car lights etc. These lights are not global uniform, thus, the glow is present in the image. Narasimhan et al [22] believed that the model of the glow is an atmospheric point spread function (APSF). Inspired by this,

1520-9210 (c) 2018 IEEE. Personal use is permitted, but republication/redistribution requires IEEE permission. See http://www.ieee.org/publications_standards/publications/rights/index.html for more information.

This article has been accepted for publication in a future issue of this journal, but has not been fully edited. Content may change prior to final publication. Citation information: DOI 10.1109/TMM.2018.2820327, IEEE Transactions on Multimedia

Li et al [17] represented the entire nighttime haze scenes by adding the glow model into the daytime haze image model:

$$X_c(p) = Z_c(p)t(p) + A_c(1 - t(p)) + A_a * APSF \tag{11}$$

where $c \in \{r, g, b\}$ indicates a color channel index, X_c indicates observed nighttime images. Z_c indicates the scene radiance vector. t is the transmission map and indicates the portion of light that penetrates through the haze. A_c indicates atmospheric light which is not globally uniform any longer. A_a indicates the active light sources, that the intensity is convolved with $APSF$. So, in order to get the scene radiance vector, that is, the haze-free image Z, the glow (that is $A_a * APSF$) are decomposed from the input image ($X_c(p)$), and the atmospheric light A_c and the transmission map t are estimated.

B. Glow Removal From the Input Image

From the unprocessed images, we can see that glow can reduce the visibility of the image or even make some objects unseen. In order to obtain a good visual image, the glow should be removed from the input image. For simplicity, the equation (11) can be rewritten as:

$$X_c(p) = J_c(p) + G_c(p) \tag{12}$$

where, $J_c(p) = Z_c(p)t(p) + A_c(1 - t(p))$, we call it a grow-free nighttime haze image, and $G_c(p) = A_a * APSF$, it is a glow image. From the equation (12), the glow removal can be regarded as a layer separation problem [23]. Because the brightness of the glow decreases gradually and smoothly, at the same time, the glow effect of the input image shares the characteristic which the gradient histogram of the smooth layer has a "short tail" [17]. So the method in [23] can be applied to separate the glow from the input image.

The objective function for glow layer separation can be defined as follow [17]:

$$\begin{aligned} E(J) &= \sum_p (\rho(J(p) * f_{1,2}) + \lambda_1((X(p) - J(p)) * f_3)^2) \\ &s.t. 0 \le J(p) \le X(p) \\ &\sum_p J_r(p) = \sum_p J_g(p) = \sum_p J_b(p) \end{aligned} \tag{13}$$

where, $f_{1,2}$ is the 2-direction first derivative filters. f_3 is the second order Laplacian filter and the operator $*$ denotes convolution. $\rho(\mu) = \min(\mu^2, \tau)$ is a robust function which preserves large gradients of the input image X in the remaining nighttime haze layer J [17]. For simplicity, we define $F^j L = L * f_j$, then, the objective function can be rewritten as:

$$E(J) = \sum_p (\rho(F^{1,2}J(p)) + \lambda_1(F^3 J(p) - F^3 X(p))^2) \tag{14}$$

According to the method [23], in order to move the $F^j L$ term outside the $\rho(\cdot)$ function, a weight β is introduced to the objective function, the new objective function can be rewritten as:

$$\begin{aligned} E(J) = \sum_p (&\beta(F^{1,2}J(p) - g^{1,2})^2 + \rho(g^{1,2}) \\ &+ \lambda_1(F^3 J(p) - F^3 X(p))^2) \end{aligned} \tag{15}$$

The solution to the above optimization problem is given as follows:

Update g^j. Keeping $J(p)$ fixed, the closed-form solution is given as

$$g^j = \begin{cases} F^j J(p), & if (F^j J(p))^2 > \tau, \\ \dfrac{\beta}{\beta + 1} F^j J(p), & otherwise. \end{cases} \tag{16}$$

It is worth noting that the closed-form solution in [23] is given as

$$g^j = \begin{cases} F^j J(p), & if (F^j J(p))^2 > \dfrac{1}{\beta}, \\ 0, & otherwise. \end{cases} \tag{17}$$

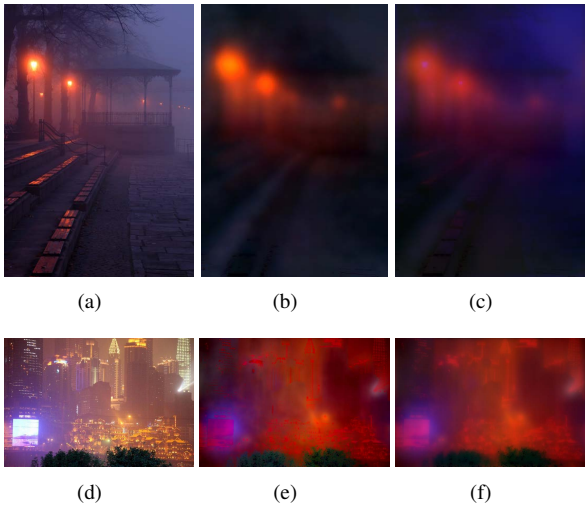

Fig. 2: (a,d) two nighttime haze images; (b,e) glow images by the method [23]; (c,f) glow images by the proposed algorithm. The glow images produced by the proposed algorithm are smoother.

It can be verified that the above solution is an approximated solution while the provided solution in the equation (16) is an exact one. Therefore, our solution is more accurate than the solution in [23].

Compute $J(p)$. With g^j fixed, as [23], we apply a 2D FFT $\mathcal{F}$ which diagonalizes the convolution matrices F^j's, then the optimal $J(p)$ can be obtained:

$$J(p) = \mathcal{F}^{-1}(A), \tag{18}$$

$$A = \frac{\beta \Sigma_j (\mathcal{F}(F^j) \star \mathcal{F}(g^j)) + \lambda_1 \mathcal{F}(F^3) \star \mathcal{F}(F^3) \mathcal{F}(X)}{\beta \Sigma_j (\mathcal{F}(F^j) \star \mathcal{F}(F^j)) + \lambda_1 \mathcal{F}(F^3) \star \mathcal{F}(F^3) + \xi} \tag{19}$$

Where $\star$ is the complex conjugate, ξ is a constant and defined as 10^{-16}, it can be used to increase the stability of the proposed algorithm. After getting the $J(p)$, it need to be normalized as [23]. Once the $J(p)$ is obtained, the glow image $G(p)$ can be finded easily.

The Fig. 2 shows the separated glow image by the algorithm in [23] and the proposed algorithm. Clearly, the glow's detail

1520-9210 (c) 2018 IEEE. Personal use is permitted, but republication/redistribution requires IEEE permission. See http://www.ieee.org/publications_standards/publications/rights/index.html for more information.

This article has been accepted for publication in a future issue of this journal, but has not been fully edited. Content may change prior to final publication. Citation information: DOI 10.1109/TMM.2018.2820327, IEEE Transactions on Multimedia

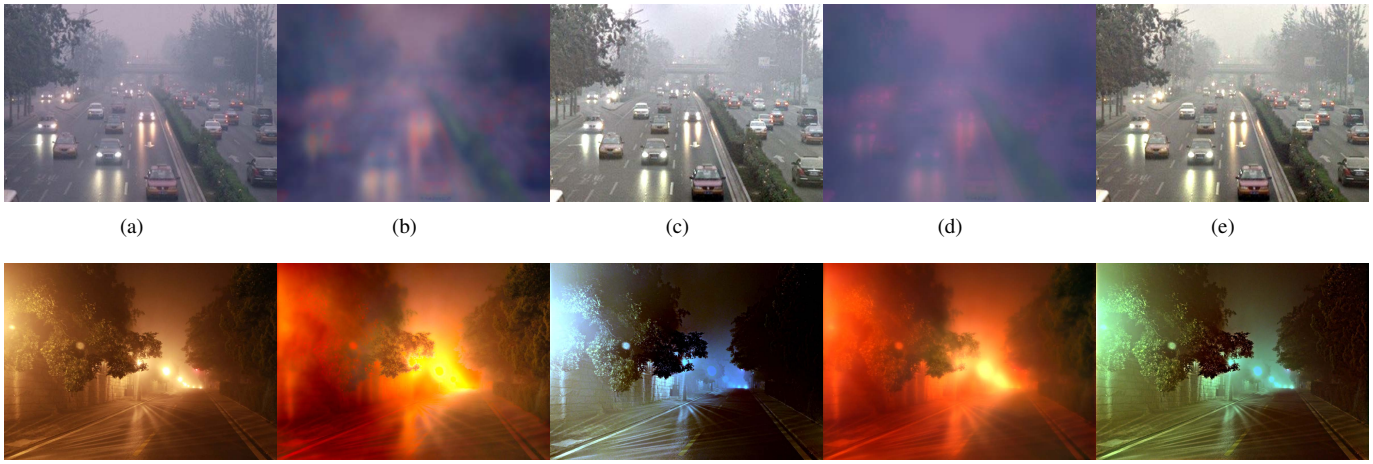

(a) (b) (c) (d) (e)

(f) (g) (h) (i) (j)

Fig. 3: (a,f) two haze images; (b,g) glow images by the method [23]; (c,h) glow-free haze images by the method [23]; (d,i) glow images by the proposed algorithm; (e,j) glow-free haze images by the proposed algorithm. There are more details in the glow-free haze images by the proposed algorithm.

in (c,f) is more meticulous and continuous than (b,e). Therefore, the proposed glow decomposition method is better than the method in [23]. Since the input image is composed of a glow image and a glow-free haze image, the process of glow decomposition directly affects the composition of glow-free image, thereby affecting the quality of dehazed image. The Fig. 3 shows the glow images and glow-free images by the Li's algorithm and our algorithm. It can be seen from the Fig. 3 (c) (e) that the glow can be removed better by our algorithm, and from the Fig. 3 (h) (j) that the glow-free haze images are closer to the nature scene.

C. Atmospheric Light Estimation

After the glow being removed from the input image, a glow-free nighttime haze image is finded. In order to restore the haze-free image, the atmospheric light A_c and the transmission map t need to be estimated. Since the models of a daytime haze image and a glow-free nighttime haze image are almost the same except for the atmospheric light, it can be expected that some existing method of daytime haze image dehazing can be applied to removal the haze from the glow-free nighttime haze image. The atmospheric light is always regarded as the brightest color in the daytime haze image. However, due to the presence of the light sources, the atmospheric light is not global uniform in the glow-free nighttime haze image.

According to the image formation model, the image $Z_c(p)$ is a produce of illumination and reflectance components:

$$Z_c(p) = A_c(p)R_c(p), \tag{20}$$

where $R_c(p)$ is the reflectance component.

The glow-free nightime haze image is then represented as

$$X_c(p) = A_c(p)R_c(p)t(p) + A_c(p)(1 - t(p)). \tag{21}$$

Same as [24], the components $A_c(p)$ and $t(p)$ are assumed to be constant in a local window of p. It can then be derived that

$$\max_{p' \in \Omega(p)} \{X_c(p')\} = A_c(p) \max_{p' \in \Omega(p)} \{R_c(p')\}t(p) + A_c(p)(1 - t(p)). \tag{22}$$

Using the following maximum reflectance prior [24],

$$\max_{p' \in \Omega(p)} \{R_c(p')\} = 1 \tag{23}$$

it can be derived that

$$A_c(p) = \max_{p' \in \Omega(p)} \{X_c(p')\}. \tag{24}$$

(a) (b) (c)

Fig. 4: (a) a glow-free haze image; (b) an initial atmospheric light image; (c) a refined atmospheric light image. There are morphological artifacts in the initial atmospheric light image and they are removed by the WGIF.

On the basis of the characteristic of super-pixel, the atmospheric light has more chance to be uniform in each super-pixel. Hence, the glow-free nighttime haze image J_c is decomposed into N super-pixels rather than a grid of small areas as in [17]. The brightest pixel in the *ith* super-pixel is regarded as the atmospheric light of the super-pixel and it is assigned to all the pixels in the super-pixel to make up the initial atmospheric light $IA_c(p)$. It can be shown in Fig. 7 that the morphological artifacts are significantly reduced using the proposed super-pixel based method. Even though the morphological artifacts are reduced using the super-pixels,

1520-9210 (c) 2018 IEEE. Personal use is permitted, but republication/redistribution requires IEEE permission. See http://www.ieee.org/publications_standards/publications/rights/index.html for more information.

This article has been accepted for publication in a future issue of this journal, but has not been fully edited. Content may change prior to final publication. Citation information: DOI 10.1109/TMM.2018.2820327, IEEE Transactions on Multimedia

there are still visible morphological artifacts. The WGIF can be adopted to remove the morphological artifacts so as to get the smooth global atmospheric light $A_c(p)$. The images to be filtered are $IA_c(p)$ and the guidance images are the color components of the glow-free nighttime haze images $J_c(p)$. Using the WGIF in the equations (5) and (6), the optimal values of a_k and b_k are computed as :

$$a_k = \frac{\mu_{J \bigodot IA,r}(k) - \mu_{J,r}(k)\mu_{IA,r}(k)}{\sigma^2_{J,r}(k) + \frac{\lambda}{\Gamma_J(k)}}, \tag{25}$$

$$b_k = \mu_{IA,r}(k) - a_k\mu_{J,r}(k) \tag{26}$$

where the value of r is selected as 60 and the value of λ is selected as 4096. The final value of $A_c(p)$ is given as:

$$A_c(p) = \bar{a}_k J_c(p) + \bar{b}_k \tag{27}$$

where $\bar{a}_k$ and $\bar{b}_k$ are obtained with average filter in the window $\Omega(p)$. As demonstrated in the Fig. 4, the morphological artifacts are indeed removed by the WGIF. It should be pointed out that the value of r is 60 using the proposed super-pixel based method. As a result, details in the areas of fine structures are preserved better.

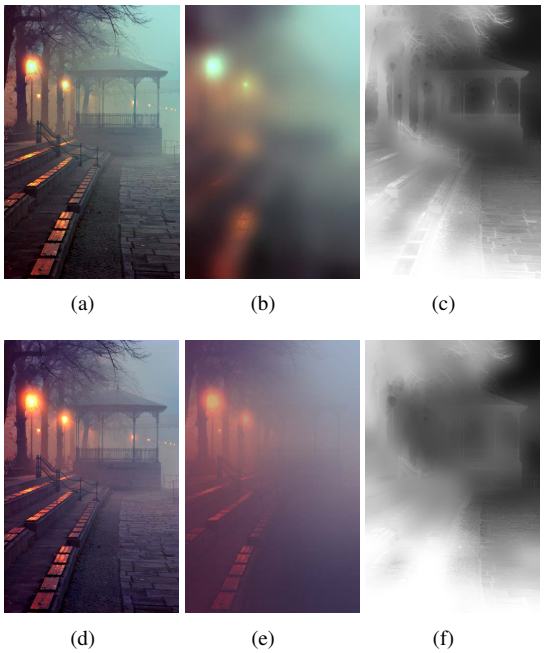

(a) (b) (c)

(d) (e) (f)

Fig. 5: (a),(b),(c) respectively is a glow-free haze image, an atmospheric light image and a transmission map by the method [17]; (d),(e),(f) respectively is a glow-free haze image, an atmospheric light image and a transmission map by the proposed method. The transmission map estimated by the proposed method matches the structure of real scene better.

The Fig. 5 (b) (e) shows the atmospheric light image by different methods. The atmospheric light image estimated by our algorithm matches the structure of the haze image better. In addition, there are fewer saturated pixels in our atmospheric light image. As such, there are fewer under-exposed pixels in the final image.

The Fig. 6 shows the atmospheric light image and dehazed image by different methods under the same glow-free image. It can be seen from the Fig. 6 (b) (e) that the atmospheric light image estimated by our algorithm is more smooth. And there are visible halo artifacts and noise is amplified in the dehazed image as (d). Therefore, the proposed algorithm can be used to process the nighttime haze image.

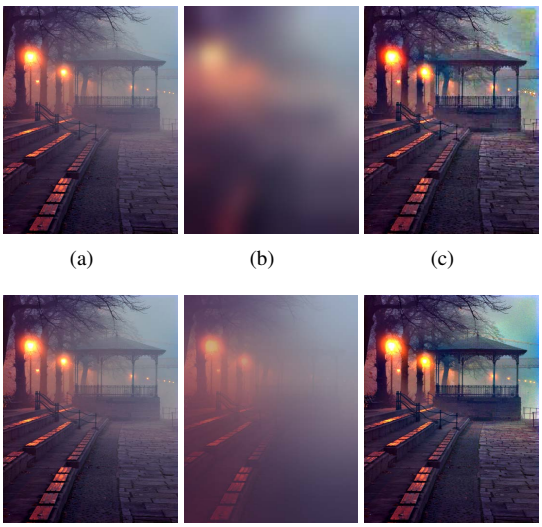

(a) (b) (c)

(d) (e) (f)

Fig. 6: (a),(d) are the same glow-free haze image by the proposed method; (b),(c) respectively is an atmospheric light image, dehazed image by the method [17]; (e),(f) respectively is an atmospheric light image, dehazed image by the proposed method.

D. Transmission Map Estimation

After getting the atmospheric light, the transmission map is estimated to recover the scene radiance. Same as the existing haze removal algorithms in [5], [16], [17], [23] [25], the proposed algorithm is on top of the dark channel [25]. However, the dark channel is not required to be 0 as by the existing haze removal algorithms in [5], [16], [17], [23] [25].

It can be derived from the equations (20) and (21) that

$$X_m(p) = Z_m(p)t(p) + (1 - t(p)), \tag{28}$$

where $X_m(p)$ and $Z_m(p)$ are defined as

$$X_m(p) = \min_{c\in\{r,g,b\}} \{\frac{X_c(p)}{A_c(p)}\}, \tag{29}$$

$$Z_m(p) = \min_{c\in\{r,g,b\}} \{\frac{Z_c(p)}{A_c(p)}\}. \tag{30}$$

Notice that the value of $t(p)$ is

$$t(p) = e^{-\alpha d(p)}, \tag{31}$$

1520-9210 (c) 2018 IEEE. Personal use is permitted, but republication/redistribution requires IEEE permission. See http://www.ieee.org/publications_standards/publications/rights/index.html for more information.

This article has been accepted for publication in a future issue of this journal, but has not been fully edited. Content may change prior to final publication. Citation information: DOI 10.1109/TMM.2018.2820327, IEEE Transactions on Multimedia

(a) (b) (c) (d) (e)

Fig. 7: (a) a glow-free nighttime haze image; (b) an initial transmission map by the method [25]; (c) a refined transmission map by the method [25]; (d) an initial transmission map by the proposed method; (e) a refined transmission map by the proposed method.

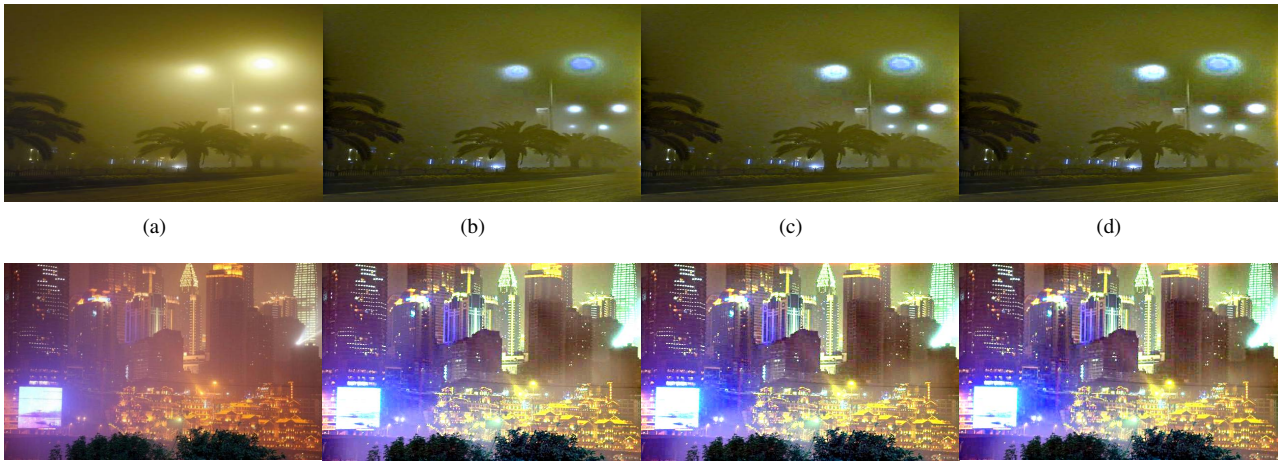

(a) (b) (c) (d)

(e) (f) (g) (h)

Fig. 8: Comparison of different number of super-pixels. (a,e) two haze images; (b,f) dehazed images with 200 super-pixels ; (c,g) dehazed images with 500 super-pixels; (d,h) dehazed images with 900 super-pixels.

and all pixels in the same superpixel S_i usually have the same depth value $d(p)$. It follows that

$$\min_{p\in S_i}\{X_d(p)\} = \min_{p\in S_i}\{Z_d(p)\}t(p) + (1 - t(p)), \tag{32}$$

where $X_d(p)$ and $Z_d(p)$ are defined as

$$X_d(p) = \min_{p'\in\Omega(p)}\{X_m(p')\}, \tag{33}$$

$$Z_d(p) = \min_{p'\in\Omega(p)}\{Z_m(p')\}. \tag{34}$$

It is worth noting that all the pixels p in the super-pixel S_i share the same $\min_{p\in S_i}\{X_d(p)\}$. Compared with the method in [9], the super-pixels are further used to reduce the variation of the first term on the right side of the equation (32). The estimation of the depth value can be improved, especially for those white objects with small or medium sizes nearby the camera. It can be observed from the above equation that the function of the dark channel is to reduce the variation range of the first term at the right side of the equation, $\min_{p\in S_i}\{Z_d(p)\}t(p)$ such that it becomes the detail layer of $\min_{p\in S_i}\{X_d(p)\}$. This is feasible due to the following reasons:

1) When the pixel p is nearby the camera, the value of $\min_{p\in S_i}\{Z_d(p)\}$ is usually very small.

2) When the pixel p belongs to the sky, the value of $t(p)$ is very small.

It is worth noting that there is exception when there are white objects with very large sizes nearby the camera. The exception is challenging for the existing haze removal algorithms.

The WGIF is then adopted to decompose the dark channel image $\min_{p\in S_i}\{X_d(p)\}$ into the base and detail layers. The guidance image is selected as Z_m. The value of $t(p)$ is then computed from the base layer. Clearly, the proposed algorithm is different from the existing dark channel prior based haze removal algorithms [5], [16], [17], [23] [25]. The dark channel is adopted to reduce the variation range of $\min_{p\in S_i}\{Z_d(p)\}t(p)$ in the proposed algorithm while the first term $\min_{p\in S_i}\{Z_d(p)\}t(p)$ is required to be cancelled by the existing dark channel prior based haze removal algorithms [5], [16], [17], [23] [25].

It is shown in the Fig. 5 (c) (f) that the transmission map estimated by the proposed method matches the structure of the nighttime haze image better than the method in [17].

The proposed transmission map estimation method is adopted to study a day-time haze image. The values of $A_c(c \in \{R,G,B\})$ are estimated using the method in [9]. It is shown in Fig. 10 that the transmission maps of all the pixels in the white house estimated by the method in [9] are very small even though the depth of the white house is small. Clearly, the values of the estimated transmission maps are not correct.

1520-9210 (c) 2018 IEEE. Personal use is permitted, but republication/redistribution requires IEEE permission. See http://www.ieee.org/publications_standards/publications/rights/index.html for more information.

This article has been accepted for publication in a future issue of this journal, but has not been fully edited. Content may change prior to final publication. Citation information: DOI 10.1109/TMM.2018.2820327, IEEE Transactions on Multimedia

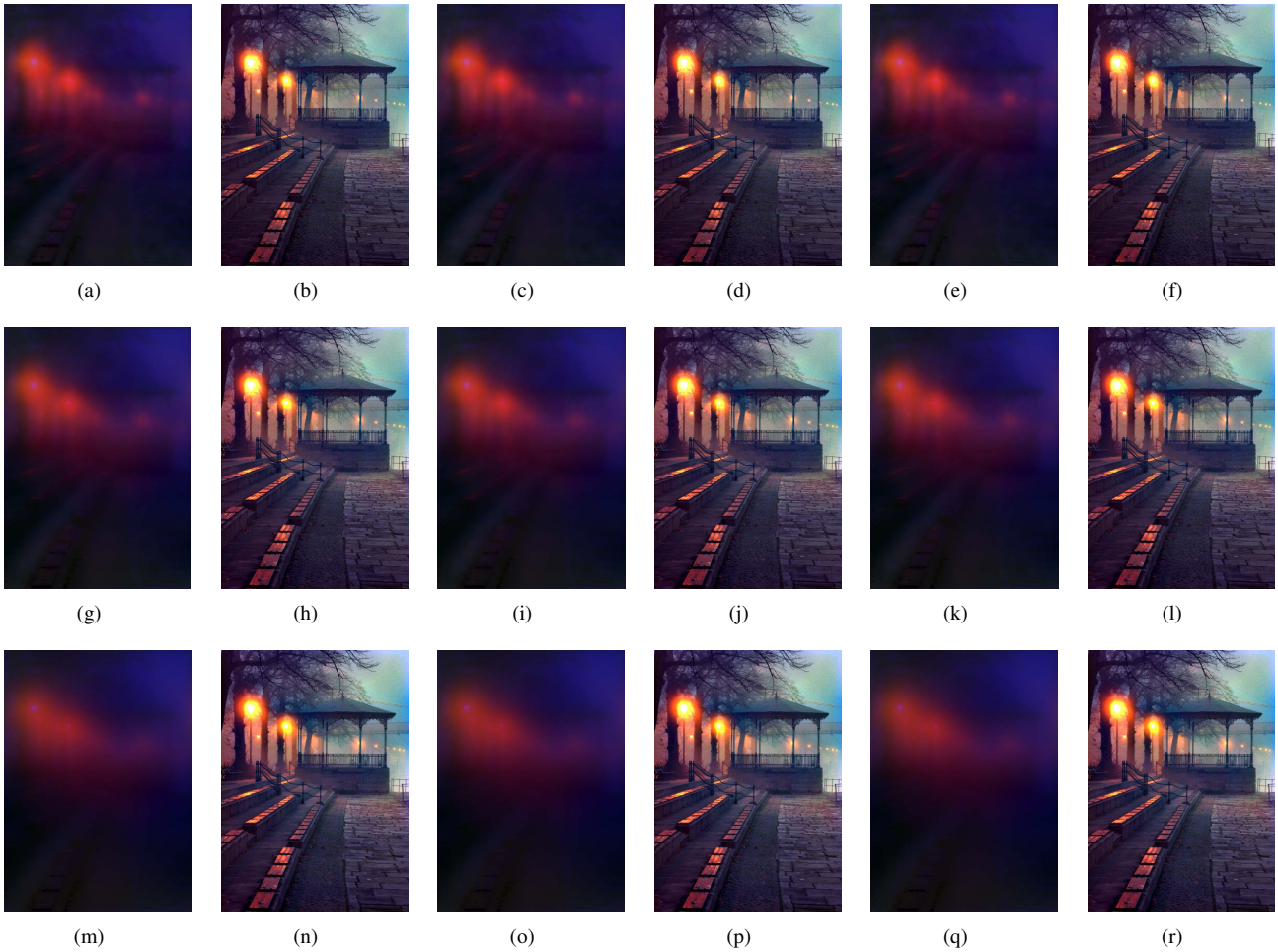

Fig. 9: The glow images and final images with different choices of (τ, λ_1) in the equations (13)-(19). (a)-(f) is respectively glow images and dehazed images with $\lambda_1 = 500$, $\tau = 1/128, 1/256, 1/512$; (g)-(l) is respectively glow images and dehazed images with $\lambda_1 = 2000$, $\tau = 1/128, 1/256, 1/512$; (m)-(r) is respectively glow images and dehazed images with $\lambda_1 = 8000$, $\tau = 1/128, 1/256, 1/512$;

Actually, this is a well known challenging problem for the existing single image haze removal algorithms. This problem is overcome by the proposed super-pixel based transmission map estimation method.

E. Recovery of the Scene Radiance

Because of the values of the global atmospheric light $A_c(p)$ and the refined transmission map $t(p)$ have already solved in the first few parts, the haze-free image $Z_c(p)$ can be recovered using the equation (35). It is worth noting that the value of t_p is always less than one. If t_p is close to zero, $Z_c(p)t(p)$ is also close to zero. In this situation, if the haze-free image is restored, the noise in the haze-free image will be significantly amplified. Thus, a lower bound t_m which was added to constrain t_p can reduce the noise. The value of the t_m is determined by the denseness of the haze. Its value is selected as 0.2 if the haze is not heavy, 0.375 otherwise. The final image is restored as

$$Z_c(p) = \frac{J_c(p) - A_c(p)}{\max(t(p), t_m)} + A_c(p) \tag{35}$$

It is worth noting that the proposed adaptation mechanism of t_m is coarse and the quality of dehazed images could be improved by a finer choice of t_m with respect to different haze levels.

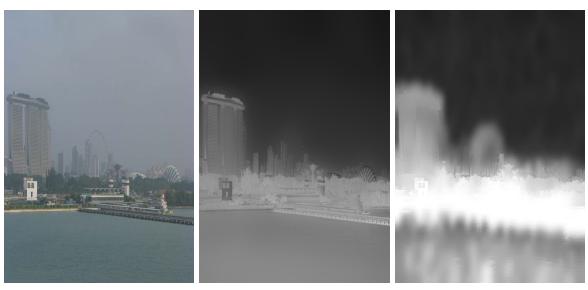

Fig. 10: (a) a day-time haze image; (b) the transmission map by the method [9]; (c) the transmission map by the proposed method.

1520-9210 (c) 2018 IEEE. Personal use is permitted, but republication/redistribution requires IEEE permission. See http://www.ieee.org/publications_standards/publications/rights/index.html for more information.

This article has been accepted for publication in a future issue of this journal, but has not been fully edited. Content may change prior to final publication. Citation information: DOI 10.1109/TMM.2018.2820327, IEEE Transactions on Multimedia

(a) (b) (c)

(d) (e) (f)

Fig. 11: The final image with different choices of (r, λ) in the equations (25)-(27) for the refinement of atmospheric light. (a) a haze image; (b) r=5, λ=4096; (c) r=20, λ=4096; (d) r=60, λ=16; (e) r=60, λ=256; (f) r=60, λ=4096.

(a) (b) (c)

Fig. 12: The final image with different choices of r in the WGIF for the refinement of transmission map. λ is defined as 1/1000, (a) r=10; (b) r=20; (c) r=60.

IV. Experimental Results

In this section, we first discuss the experimental results on the impact of different number of super-pixels and r and λ in the WGIF. Besides, the experimental result is compared with different choices of (τ, λ_1) in the equations (13)-(19). Then we compare the proposed algorithm with the daytime haze removal algorithms in [5] and four nighttime haze removal algorithms in [16] [17] [20] and [24].

A. Different Choices of Parameters

In our algorithm, the number of the super-pixel N is one key parameter. This is because that N plays an important role in the estimation of atmospheric light and transmission map. So the effect of different super-pixel number is evaluated in this subsection. As illustrated in the Fig. 8, as the number of super-pixel increasing, the quality of the final image is improved. There are more details in the final image and haze is also removed better. Otherwise, there are visible morphological artifacts. On the other hand, the running time of the proposed algorithm becomes longer when the the number of super-pixel increase due to the SLIC. In order to obtain a good tradeoff between the running time and the quality of the final image, the number N is set 900 in this paper.

As shown in the Fig. 9, if the value of λ_1 is too small, the glow image is not enought smooth, and the details are not well preserved. If the value of λ_1 is too larger, haze is not removed well in the final image. In order to obtain a good experiment results, the number λ_1 is set 2000, $\tau = 1/256$ in this paper.

(a) (b) (c)

Fig. 13: (a) haze image; (b) dehazed image by the method in [20]; (c) dehazed image when super-pixel do not perform well in segmentation.

Two more important parameters are r and λ for the refinement of transmission map and refinement of atmospheric light in the equations (25)-(27). As shown in the Fig. 11 that there are halo artifacts in the final image if the value of r is too small and haze is not removed well in the final image if the value of λ is too small. From the Fig. 12, we can see that, when r is defined 20, the effect of dehazing works better. So, if not specified in this paper, the values of r and λ are selected as 60 and 4096 for the refinement of atmospheric light, and, the values of r and λ are selected as 20 and 1/1000 for the refinement of transmission map.

It should be pointed out that the SLIC in [21] might not perform well if a hazed image is too noisy. One example is given in Fig. 13. Subsequently, there will be morphological artifacts in the dehazed image, as the Fig. 13 (c).

B. Comparison Among Different Haze Removal Algorithm

For comparison, the results using dehazing algorithms in [5], [16], [17], [20], [24] and our algorithm are shown in the Fig. 14, Fig. 15, and Fig. 16. He's method in [5] is a classical algorithm for daytime haze images. It is not surprised that it is not suitable to remove the haze from a nighttime haze image. Only part of haze can be removed by this method and the glow still exists in the final images. The methods in [16] and [17] are designed for nighttime haze images. Although the method [16] can remove the glow and most of the haze from the nighttime haze images, there are visible halo artifacts and noise is amplified in the dehazed images as illustrated in the Fig. 14 (h), (m). In addition, there are visible glow around the light sources. The method in [17] works better than the method in [16]. Unfortunately, noise is also amplified and halo artifacts still exists in the final images. The algorithm in [17] accounts that the atmospheric light is locally constant in a

1520-9210 (c) 2018 IEEE. Personal use is permitted, but republication/redistribution requires IEEE permission. See http://www.ieee.org/publications_standards/publications/rights/index.html for more information.

This article has been accepted for publication in a future issue of this journal, but has not been fully edited. Content may change prior to final publication. Citation information: DOI 10.1109/TMM.2018.2820327, IEEE Transactions on Multimedia

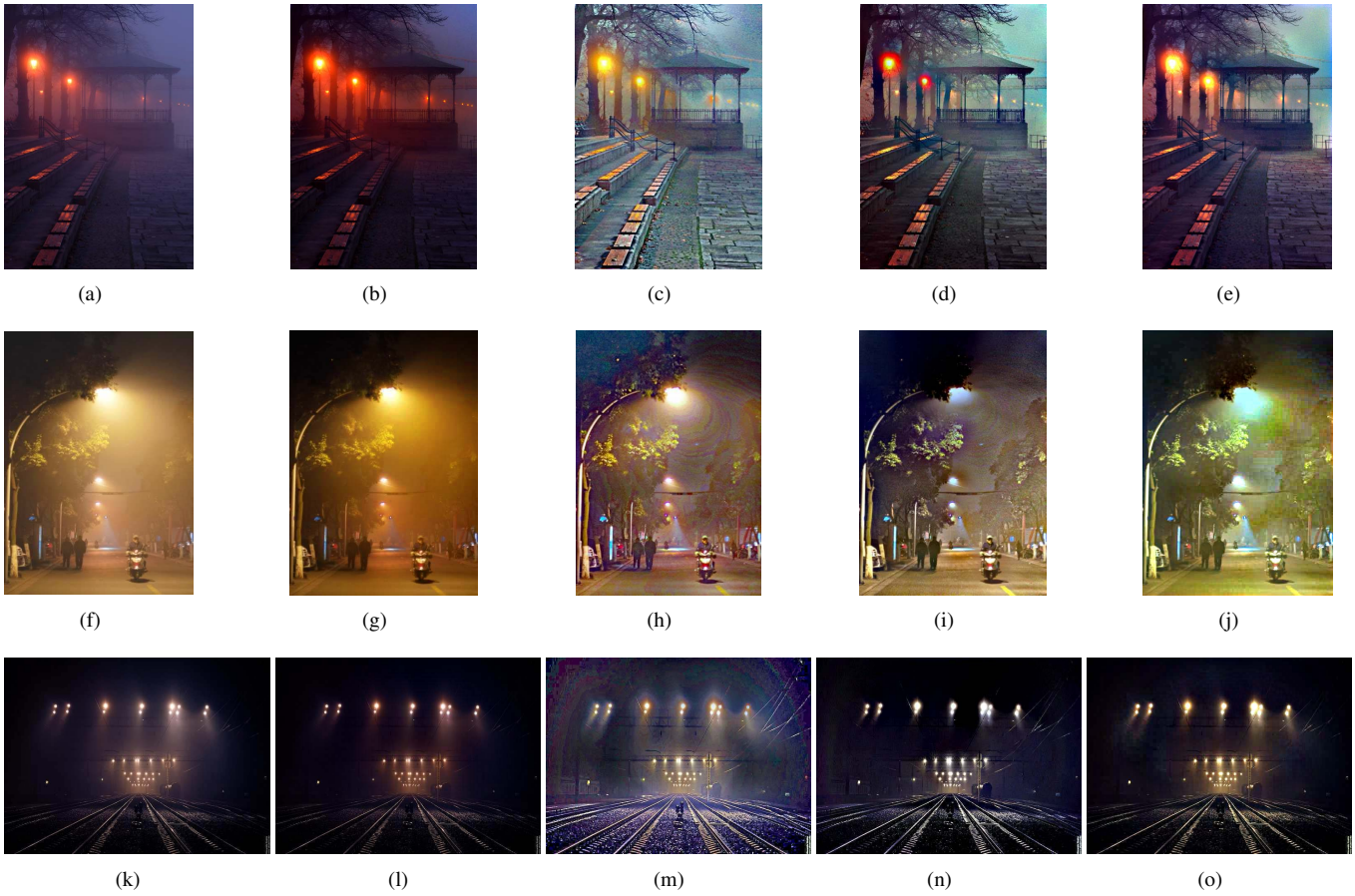

Fig. 14: (a,f,k) haze images; (b,g,l) dehazed images by the method in [5]; (c,h,m) dehazed images by the method in [16]; (d,i,n) dehazed images by the method in [17]; (e,j,o) dehazed images by the proposed algorithm.

grid of small area. However, this is not always true. On the other hand, according to features of the super-pixels, it is more likely that the atmospheric light is constant in the super-pixel.

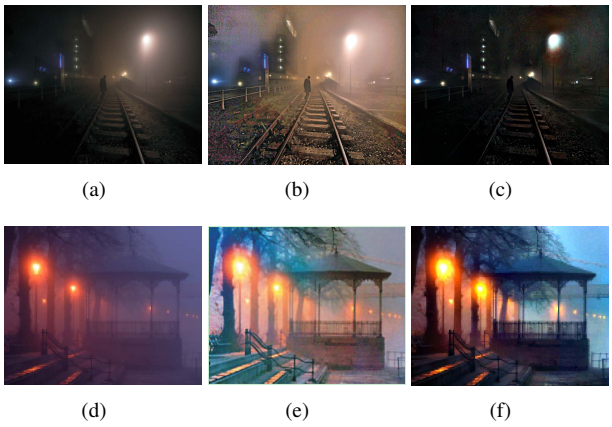

Fig. 15: (a,d) haze images; (b,e) dehazed images by the method in [20]; (c,f) dehazed images by the proposed algorithm.

As illustrated in the Fig. 15 (b), although the method in [20] can remove most of the haze from the nighttime haze images, there is color distortion in the dehazed images such as regions of branches. The method in [16] was improved as in [24].

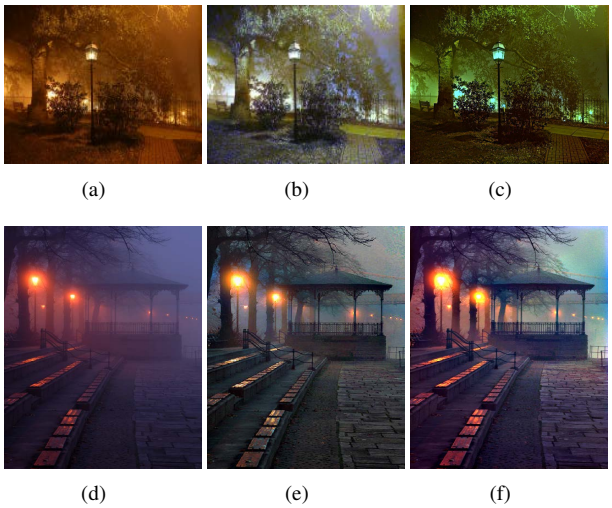

Fig. 16: (a,d) haze images; (b,e) dehazed images by the method in [24]; (c,f) dehazed images by the proposed algorithm.

In the Fig. 16, the proposed algorithm is further compared with the method [24]. The algorithm in [24] usually performs well except for very few cases with color distortion such as

1520-9210 (c) 2018 IEEE. Personal use is permitted, but republication/redistribution requires IEEE permission. See http://www.ieee.org/publications_standards/publications/rights/index.html for more information.

This article has been accepted for publication in a future issue of this journal, but has not been fully edited. Content may change prior to final publication. Citation information: DOI 10.1109/TMM.2018.2820327, IEEE Transactions on Multimedia

the regions of grasses and leaves in Fig. 16 (b). Neither the algorithm in [20] nor the algorithm in [24] addressed the glow artifacts. As such, the glow artifacts are more visible in the dehazed images by the algorithms in [20] and [24].

It is worth noting that a larger t_m is selected in the equation (35) to avoid amplifying noise in the sky regions. On the other hand, fine details could also be smoothed by the proposed algorithm. It is desired to design a finer t_m for the proposed algorithm. In spite of our algorithm works well in dehazing of nighttime haze image, there are still some deficiencies. For example, the haze removal image looks darker than the input image. Fortunately, this problem can be addressed using a single image brightening algorithm in [26]. The running time of the proposed algorithm is slightly longer due to segment the glow-free image into super-pixels.

V. Conclusion

This paper presented a novel super-pixel based nighttime haze image dehazing algorithm. The proposed algorithm can remove the glow and the haze better than the state-of-the-art methods. Local fine details are also preserved better, and the color distortion and halo artifacts are obviously reduced. As such, the haze-free image is closer to a nature scene.On the other hand, because segmentation of glow-free nighttime haze images into super-pixels is required by the proposed algorithm, the running time and the algorithm's complexity are increased. It is known that the existing single image haze removal algorithms suffer from amplifying noise in the sky region. This problem could be addressed by choosing a finer adaptive t_m in the equation (35). This problem will be studied in our future research.

Acknowledgment

This work is supported by National Natural Science Foundation of China (NSFC) (No. 61773106, No. 61703086).

References

[1] S. G. Narasimhan and S. K. Nayar, "Vision and the atmosphere," *International Journal on Computer Vision*, vol. 48, no. 3, pp. 233-254, Jun. 2002.

[2] Y. Y. Schechner, S. G. Narasimhan, and S. K. Nayar, "Polarization based vision through haze," *Applied Optics*, vol. 42, no. 3, pp. 511-525, 2003.

[3] Y. H. Lai, Y. L. Chen, C. J. Chiou, and C. T. Hsu, "Single-image dehazing via optimal transmission map under scene priors," *IEEE Transactions on Circuit and Systems for Video Technology*, vol. 25, no. 1, pp. 1-14, Jan. 2015.

[4] W. C. Wang, X. H. Yuan, X. J. Wu, and Y. L. Liu, "Fast Image Dehazing Method Based on Linear Transformation," *IEEE Transactions on Multimedia*, vol. 19, no. 6, pp. 1142-1155, Jun. 2017.

[5] K. M. He, J. Sun, and X. O. Tang, "Guided image filtering," *IEEE Transactions on Pattern Analysis and Machine Intelligence*, vol. 35, no.6, pp. 1397-1409, Jun. 2013.

[6] F. Kou, W. H. Chen, C. Y. Wen, and Z. G. Li, "Gradient Domain Guided Image Filtering," *IEEE Transactions on Image Processing*, vol. 24, no.11, pp. 4528-4539, Nov. 2015.

[7] Z. G. Li, J. H. Zheng, W. Yao, and Z. J. Zhu, "Single image haze Removal via a simplified dark channel," in *2015 IEEE International Conference on Acoustics, Speech and Signal Processing*, pp. 1608-1612, Apr. 2015.

[8] Q. S. Zhu, D. Wu, Y. Q. Xie, and L. Wang, "Quick shift segmentation guided single image haze removal algorithm," *Proceedings of the 2014 IEEE International Conference on Robotics and Biomimetics*, pp. 113-117, Dec. 2014.

[9] Z. G. Li and J. H. Zheng, "Edge-preserving decomposition-based single image haze removal," *IEEE Transactions on Image Processing*, vol. 24, no. 12, pp. 5432-5441, Dec. 2015.

[10] M. M. Yang, J. C. Liu and Z. G. Li, "Super-pixel based single image haze removal," *Proceedings of the 28th Chinese Control and Decision Conference, CCDC 2016*, pp. 1965-1969, Aug. 2016.

[11] Z. G. Li, J. H. Zheng, Z. J. Zhu, W. Yao, and S. Q. Wu, "Weighted guided image filtering," *IEEE Transactions on Image Processing*, vol. 24, no. 1, pp. 120-129, Jan. 2015.

[12] H. T. Xu, G. T. Zhai, X. L. Wu, and X. K. Yang, "Generalized Equalization Model for Image Enhancement," *IEEE Transactions on Multimedia*, vol. 16, no. 1, pp. 61-82, Jan. 2014.

[13] K. T. Shih and H. H. Chen, "Exploiting Perceptual Anchoring for Color Image Enhancement," *IEEE Transactions on Multimedia*, vol. 18, no. 2, pp. 300-310, Feb. 2016.

[14] F. Kou, Z. Wei, W. H. Chen, X. M. Wu, C. Y. Wen, and Z. G. Li, "Intelligent detail enhancement for exposure fusion," *IEEE Transactions on Multimedia*, Aug. 2017.

[15] S. C. Pei and T. Y. Lee, "Nighttime haze removal using color transfer pre-processing and dark channel prior," *IEEE International Conference on Image Processing*, pp. 957-960, Oct. 2012.

[16] J. Zhang, Y. Cao, and Z. Wang, "Nighttime haze removal based on a New Imaging Model," *IEEE International Conference on Image Processing*, pp. 4557-4561, Oct. 2014.

[17] Y. Li, R. T. Tan, and M. S. Brown, "Nighttime haze removal with glow and multiple light colors," *IEEE International Conference on Computer Vision*, pp. 226-234, Dec. 2015.

[18] Z. G. Li and J. H. Zheng, "Single Image De-Hazing Using Globally Guided Image Filtering," *IEEE Transactions on Image Processing*, vol. 27, no. 1, pp. 442-450, Jan. 2018.

[19] L. K. Choi, J. You, and A. C. Bovik, "Referenceless prediction of perceptual fog density and perceptual image defogging," *IEEE Transactions on Image Processing*, vol. 24, no. 11, pp. 3888-3901, Nov. 2015.

[20] C. Ancuti, C. O. Ancuti, C. De Vleeschouwer, and A. C. Bovik, "Night-time dehazing by fusion," *IEEE International Conference on Image Processing*, pp. 2256-2260, 2016.

[21] R. Achanta, A. Shaji, K. Smith, A. Lucchi, and P. Fua, "SLIC superpixels compared to state-of-the-art superpixel methods," *IEEE Transactions on Pattern Analysis and Machine Intelligence*, vol. 34, no. 11, pp. 2274-2282, Nov. 2012.

[22] S. G. Narasimhan and S. K. Nayar, "Shedding light on the weather," *IEEE Conference Computer Vision and Pattern Recognition*, 2003.

[23] Y. Li and M. S. Brown, "Single image layer separation using relative smoothness," *IEEE Conference Computer Vision and Pattern Recognition*, 2014.

[24] J. Zhang, Y. Cao, S. Fang, Y. Kang, and C. W. Chen, "Fast haze removal for nighttime image using the reflectance prior," in *2017 Conference on Computer Vision and Pattern Recognition*, Jul. 2017.

[25] K. M. He, J. Sun, and X. O. Tang, "Single image haze removal using dark channel prior," *IEEE Transactions on Pattern Recognition and Machine Intelligence*, pp. 2341-2353, 2011.

[26] Z. G. Li and J. H. Zheng, "Single image brightening via exposure fusion," in *2016 IEEE International Conference on Acoustics, Speech and Signal Processing*, pp. 1756-1760, Shanghai, China, Mar. 2016.

[27] F. Liu, C. Shen, G. Liu, and I. Reld, "Learning Depth from Single Monocular Images Using Deep Convolutional Neural Fields," *IEEE Transactions on Pattern Analysis and Machine Intelligence*, vol. 38, no. 10, pp. 2024-2039, Dec. 2016.

Minmin Yang received the B.Eng and M.Eng degree from University of Jinan, Jinan, China, in 2011, 2014, respectively. She is currently pursuing the PhD degree in control theory and control engineering at Northeastern University, Shenyang. Her current research interests include image and video processing.

1520-9210 (c) 2018 IEEE. Personal use is permitted, but republication/redistribution requires IEEE permission. See http://www.ieee.org/publications_standards/publications/rights/index.html for more information.

This article has been accepted for publication in a future issue of this journal, but has not been fully edited. Content may change prior to final publication. Citation information: DOI 10.1109/TMM.2018.2820327, IEEE Transactions on Multimedia

Jianchang Liu received the B.Eng, M.Eng, and PhD degree from the northeastern university china in 1984, 1989, 1998, respectively. He is now a professor at the School of Information Science and Engineering, Northeastern University. He was the dean of the school of Information Science and Engineering from 2004-2015. He was the president of the Qinhuangdao branch of Northeastern University since 2015. He has published more than 90 papers by premier conferences and journals.

His research interest covers image and video processing, modeling, control and optimization for complex process, fault diagnosis, intelligent control theory and application.

Zhengguo Li (SM'03) received the B.Sci and M.Eng from Northeastern University, Shenyang, China, in 1992 and 1995, respectively, and the Ph.D. degree from Nanyang Technological University, Singapore, in 2001.

His current research interests include computational photography, mobile imaging, video processing & delivery, and switched and impulsive control. He has co-authored one monograph, more than 200 journal/conference papers including more than 40 IEEE Transactions, and ten granted USA patents, including normative technologies on scalable extension of H.264/AVC and HEVC. He has been actively involved in the development of H.264/AVC and HEVC since 2002. He had three informative proposals adopted by the H.264/AVC and three normative proposals adopted by the HEVC. Currently, he is with the Agency for Science, Technology and Research, Singapore. He is a member of SIG on computational imaging. He served a General Chair of IEEE ICIEA in 2016, a Technical Brief Co-Founder of SIGGRAPH Asia, a General Co-Chair of CCDC in 2013, leading Workshop Chair of IEEE ICME in 2013, and an Area Chair of IEEE ICIP 2016. He was an Associate Editor of IEEE Signal Processing Letters from 2014-2016 and is an Associate Editor of IEEE Transactions on Image Processing Since 2016.

1520-9210 (c) 2018 IEEE. Personal use is permitted, but republication/redistribution requires IEEE permission. See http://www.ieee.org/publications_standards/publications/rights/index.html for more information.